THE AMERICAN MINERALOGIST, VOL. 46, NOVEMBER–DECEMBER, 1961

MONTMORILLONITE: HIGH TEMPERATURE REACTIONS AND CLASSIFICATION

R. E. GRIM AND GEORGES KULBICKI,* *University of Illinois, Urbana, Illinois.*

ABSTRACT

About forty samples of the montmorillonite group of clay minerals were heated to an elevated temperature (1400° C.) and the phase transformations studied by continuous *x*-ray diffraction. Chemical, cation exchange, differential thermal, infra-red, and optical data were obtained also on the samples.

All of the analytical data indicate that the dioctahedral montmorillonites do not form a single continuous isomorphic series. Two different aluminous types have been found, Cheto- and Wyoming-types, which differ primarily in the population of their octahedral layers. Also, it is suggested that some (probably a small number) of the silica-tetrahedra are inverted in the Cheto-type montmorillonite. Cation exchange capacity and other properties are also not the same for the two types.

Some bentonites are mixtures of discrete particles of the two types which can be separated by particle size fractionation.

The high-temperature phase transformations of montmorillonite show large variations depending on the composition and structure of the original material. The transformations are discussed in detail.

INTRODUCTION

The object of the investigation reported herein was to study the successive structural changes taking place when members of the montmorillonite group of clay minerals are heated to their fusion temperature. It was thought that the results of such a study would provide a better understanding of the structure of montmorillonites and the possible variations in their compositions. It was thought also that new light might be obtained on the general matter of solid state reactions in the layer silicates.

The major technique used was continuous high temperature *x*-ray diffraction using a spectrometer. This involved mounting a furnace in the position of the specimen holder in the *x*-ray unit with some manner of controlling and recording the temperature of the furnace. This method has advantages in comparison with a technique that involves heating, then cooling, followed by *x*-ray analysis in that it eliminates uncertainties concerning possible phase changes on cooling. Further it permits the study of the rate of development of new phases, and it is relatively rapid. In some cases *x*-ray diffraction recordings with a camera also were made on quenched samples to check the spectrometer data. The *x*-ray diffraction data were supplemented by differential thermal

* Currently Director of Geological Research, Société Nationale de Pétroles d'Aquitaine, Pau, France.

analyses carried to about 1400° C., infra-red absorption data, and optical determinations. Complete silicate analyses and cation exchange capacities were obtained for the samples.

The montmorillonite clay minerals are very common, being found in many soils, sediments, and hydrothermal alteration products. They are generally the dominant constituents of bentonites. The minerals of this group have a unique, so-called expandable lattice, which has a variable *c*-axis dimension depending on the thickness of layers of water molecules between silicate layers. The structure suggested by Hofmann, Endell, and Wilm (1933), Fig. 1, is made up of silicate layers consisting of two silica tetrahedral sheets tied together through a central sheet containing aluminum and/or magnesium, iron, and occasionally other elements in octahedral coordination. The silicate layers are continuous in the *a* and *b* directions and stacked one above another in the *c* direction with variable water layers between them. As first emphasized by Marshall (1935) and Hendricks (1942), a wide variety of substitutions in octahedral and tetrahedral positions are possible within the structure, and they always leave it with a net negative charge which is satisfied externally by cations which are exchangeable.

The foregoing structure is not accepted by all investigators. Thus, Deuel *et al.* (1950) believe that they have evidence that some of the tetrahedra of the silica sheets are inverted—an idea suggested earlier by Edelman and Favajee (1940). Other ideas concerning the montmorillonite structure have been published (McConnell, 1950), but the concept originating with Hofmann *et al.* (1933) is generally accepted as depicting the most probable framework of the mineral.

The substitution of various cations for aluminum in octahedral coordination can be essentially complete, in which case specific names are applied for example, nontronite (iron), saponite (magnesium). Ross and Hendricks (1945) have shown that there is considerable variation in composition within the aluminous montmorillonites.

Recently it has been suggested that some aluminous montmorillonites that appear to be single species are in fact complex mixtures. Thus, Byrne (1954) stated that the montmorillonites he studied were mixed-layer sequences in which adjacent layers differed from one another in composition and structure. Jonas (1955) concluded that montmorillonites showing dual dehydroxylation reactions are mixtures of two forms of the mineral, and McAtee (1958) concluded that the Wyoming bentonites he studied contained a sodium montmorillonite fraction and a calcium-magnesium montmorillonite fraction, and that these fractions were a consequence of differences in isomorphic substitution within the montmorillonite crystal lattice. One of the objectives of the present

study was to investigate the possible mixing of aluminous montmorillonites in bentonites.

The montmorillonite minerals have interesting plastic, colloidal, and other properties which frequently are quite different from one sample of the mineral to another. These differences cannot in many cases now be explained either by differences in the composition of the exchangeable cations or of the silicate layer, or by present concepts of the structure. Thus, some montmorillonites have catalytic properties towards certain organic substances, whereas others do not. It follows that there is much

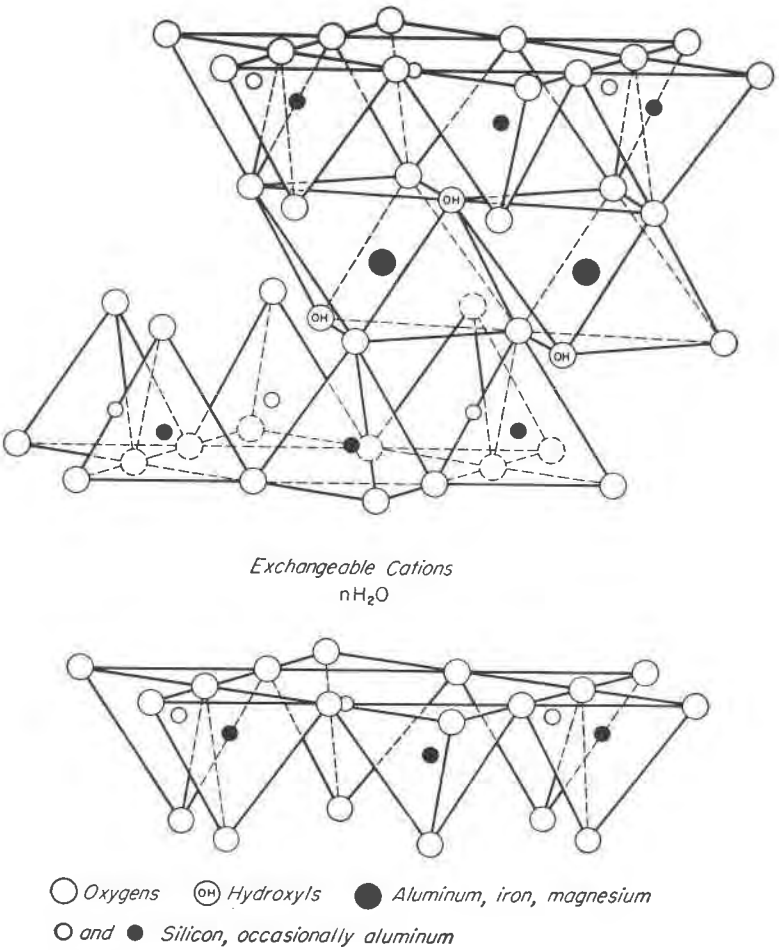

FIG. 1. Diagramatic sketch of the structure of montmorillonite according to Hofmann, Endell and Wilm (1933), Marshall (1935), and Hendricks (1942).

to be learned concerning the structure and compositional variations in this important group of minerals.

Procedure

Over a period of many years, *x*-ray diffraction diagrams of powders and oriented aggregates and differential thermal analyses have been obtained for several hundred samples of bentonites and other clays containing montmorillonite from all over the world that are in the University of Illinois collections. Preliminary studies of the high temperature reactions by continuous *x*-ray diffraction techniques were made also on many of these samples. Based on these data, about forty samples were selected for the present study which appeared to be substantially pure montmorillonite or montmorillonite plus small amounts of quartz or cristoballite. These samples were selected also to represent the variations in characteristics shown in the preliminary analyses. No claim is made that all types of montmorillonite are represented, but it is believed that there is good coverage of the aluminous variety.

Kulbicki and Grim (1957) have shown that the high temperature phases developed on heating montmorillonite are influenced greatly by the nature of the exchange cation composition. To study the relation of the montmorillonite itself to high temperature reactions it was necessary to prepare all samples with the same exchangeable cation composition. It was also deemed necessary to use material of about the same particle size, and in some cases to purify the samples. Accordingly, the following preparation procedure was followed for all samples:

The clays were dispersed in deionized water without the use of a chemical additive. If dispersion was difficult, the initial water was extracted through a porcelain filter candle, and new water added until dispersion was attained. The portion of the suspension containing the less than two micron fraction was separated by repeated decantations. Hydrochloric acid in concentrations kept less than 0.1 normal was added to the suspension containing the less than two micron particles. Within ten to twenty minutes after the addition of the acid, filtration of the clay on Buchner funnels was started. The clay was washed with acid of the same concentration until the total amount of acid to which the clay was subjected equalled about five times that necessary for complete cation exchange. This was followed by washing with deionized water until the concentration of salts in the wash water was about 1 part in 100,000.

A concentrated slurry of the material as prepared above was used to prepare oriented aggregates (Grim, 1934) for *x*-ray and optical study. The remainder of the sample was dried at room temperature for the other analyses. In cases where the influence of added cations were to be studied,

the prepared clay was not dried. Also, the cation exchange capacities were made on samples which had not been acid treated.

For high temperature *x*-ray diffraction study, oriented aggregate samples were prepared on platinum plates. The furnace used was of the design described by Kulbicki and Grim (1957). Runs were made with continuous heating at various rates, and also by soaking the samples at various temperatures. In many cases supplementary data were obtained by heating the samples in an electric furnace to various temperatures, air quenching, and then obtaining powder camera diffraction data.

Differential thermal analyses were made in a furnace with platinum wire as the heating element of the general design of Grim and Rowland (1942) with a platinum block as the sample holder. The analyses were made up to about 1400° C.

The other analyses were made by standard and well known procedures.

Location of Samples Studied

The location of each sample studied in detail is given in Table 1. No mention is made of the stratigraphic position or geologic setting of the samples although pertinent information for most of the samples has been obtained either by field studies of one of us (R.E.G.) or from the literature. Possible correlations of the character of the montmorillonite with its occurrence and mode of formation will be considered separately in a later report. All samples of the aluminous montmorillonites except possibly 6, 23, and 31 are bentonites in that their origin is by the alteration of volcanic ash in situ. The origin of the exceptions and the other montmorillonite samples is not established.

High Temperature Phase Development

Figures 2 to 7 show the high temperature phases developed when each of the samples is heated to a temperature causing the beginning of fusion. In these figures the intensity of a characteristic diffraction line is plotted against the temperature of the sample.

The data reported in Figs. 2 to 7 were obtained on samples whose temperature was continuously increased at a rate of 5° C. per minute. Other heating rates were used also on various samples, but the rate of 5° C. per minute was most satisfactory to permit the detection of the first appearance of a new phase and to record its development.

Differential thermal analyses to 1000° C. were made on all samples and for many of them the analyses were carried to 1400° C. The results of these analyses are given in Figs. 8 to 13.

The high temperature data show that all of the montmorillonites do

not develop the same crystalline phases on heating. A study of the data indicate that the highly aluminous samples investigated can be grouped into several types based on the characteristic high temperature phases developed, or as mixtures of these types. The types will be discussed separately.

TABLE 1. LOCATION OF SAMPLES

The aluminous montmorillonites are listed according to types as determined by the present study.

Cheto-type montmorillonites
1. Cheto, Arizona
2. Otay, California
3. Burrera, Jachal, San Juan, Argentina
4. El Retamito, Retamito, San Juan, Argentina
5. Mario Don Fernando, Retamito, San Juan, Argentina
6. Tatatilla, Vera Cruz, Mexico
7. Itoigawa, Niigata Prefecture, Japan

Wyoming-type montmorillonites
8. Hojun Mine, Gumma Prefecture, Japan
9. Tala, Heras, Mendoza, Argentina
10. Crook County, Wyoming
11. Rokkaku, Yamagata Prefecture, Japan
12. Amory, Mississippi
13. Santa Elena, Potrerillos, Mendoza, Argentina
14. San Gabriel, Potrerillos, Mendoza, Argentina
15. Emilia, Calingasta, San Juan, Argentina
16. Sin Procedencia, Argentina

Wyoming-type montmorillonites containing free silica
17. Usui Mine, Gumma Prefecture, Japan
18. Yakote, Akita Prefecture, Japan
19. Rokkaku, Yamagata Prefecture, Japan
20. Wayne, Alberta, Canada
21. Dorothy, Alberta, Canada
22. Cole Mine, Gonzales County, Texas
23. Cala Aqua Mine, Island of Ponza, Italy

Mixtures of Cheto- and Wyoming-type montmorillonites
24. Pembina, Manitoba, Canada
25. Polkville, Mississippi
26. Grand Junction, Colorado
27. Fadli, Mostaganem, Algeria
28. Taourirt, Morocco
29. Marnia, Algeria
30. Marnia, Algeria
31. Montmorillon, France
32. Yokote, Akita Prefecture, Japan

Miscellaneous aluminous montmorillonites
33. Colony, Wyoming
34. Amory, Mississippi
35. Weston County, Wyoming
36. Humber River, New South Wales, Australia

Iron-rich montmorillonite
37. Aberdeen, Mississippi
38. Santa Rosalina, Baja California

Nontronite
39. Manito, Washington

Hectorite
40. Hector, California

Saponite
41. Ksabi, Morocco

Talc
42. Gouverneur, New York

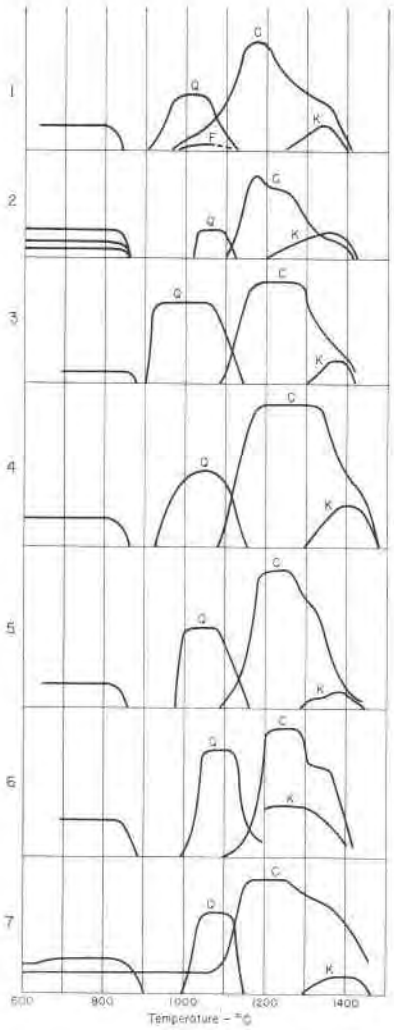

FIG. 2. High temperature phases developed on heating Cheto-type montmorillonites; Samples 1–7; Q, Beta Quartz; C, Beta Cristobalite; K, Cordierite; F, Feldspar.

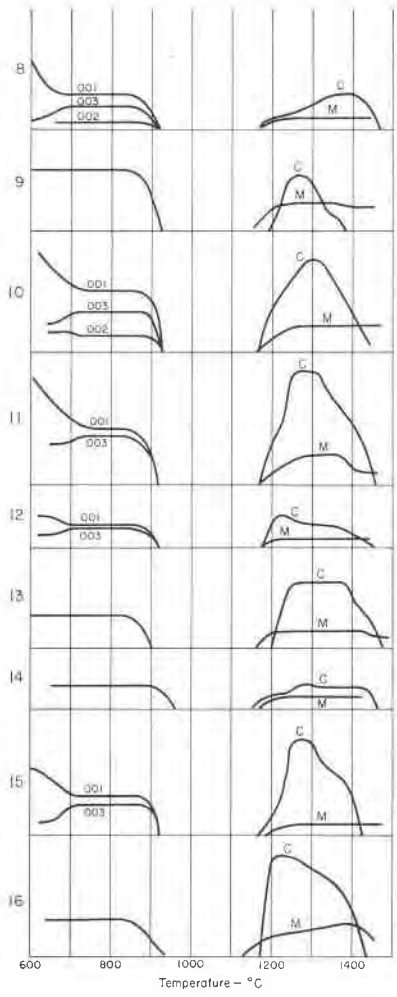

FIG. 3. High temperature phases developed on heating Wyoming-type montmorillonites; Samples 8–16; C, Beta Cristobalite; M, Mullite.

Cheto-Type

This type is so named because samples from the Cheto bentonite producing area in Arizona show very well its characteristics. Figure 2 illustrates the high temperature *x*-ray diffraction data for samples 1–7

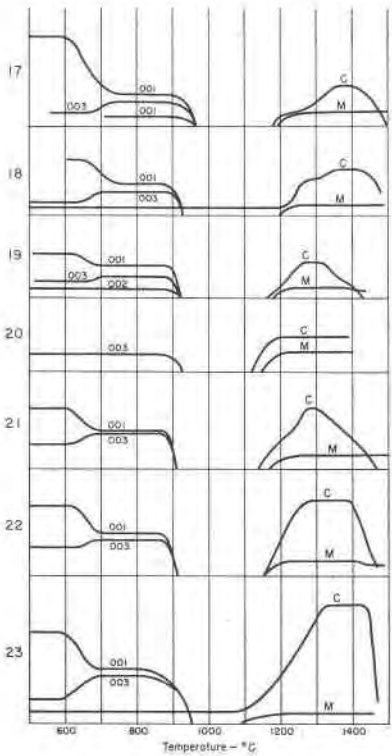

FIG. 4. High temperature phases developed on heating samples containing Wyoming-type montmorillonite plus free silica; Samples 17–23; C, Beta Cristobalite; M, Mullite.

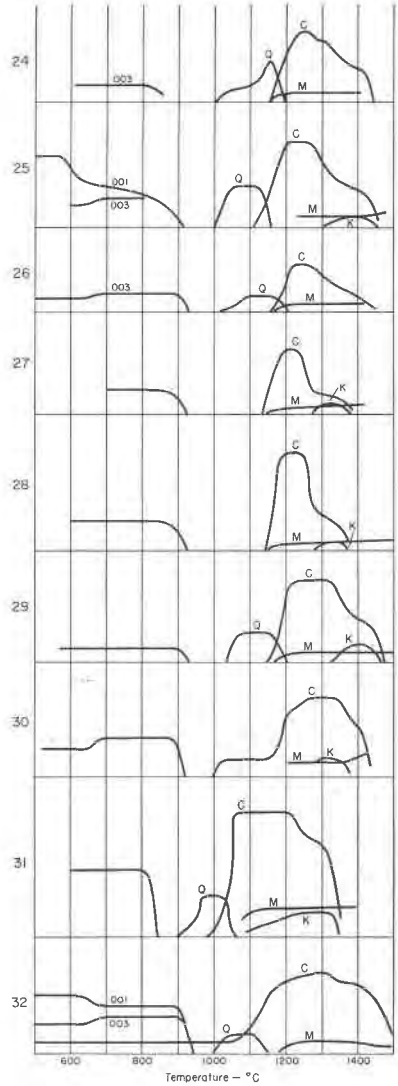

FIG. 5. High temperature phases developed on heating samples containing a mixture of Cheto-type and Wyoming-type montmorillonites; Samples 24–32; Q, Beta Quartz; C, Beta Cristobalite; M, Mullite; K, Cordierite.

showing the development of beta quartz, beta cristobalite, and cordierite, which are the characteristic high temperature crystalline phases for Cheto-type montmorillonite. Figure 8 shows the differential thermal analytical curves for the same samples.

The montmorillonite structure is preserved to 850°–900° C. where it is lost abruptly in a temperature interval of about 50° C. There does not seem to be any change in the intensity of the basal orders of the montmorillonite prior to the loss of structure.

The first high temperature phase to appear is beta quartz between about 900° C. and 1000° C. It develops at a temperature 50° to 125° higher than that for the loss of the montmorillonite structure. During the intervening interval the samples show no *x*-ray diffraction effects. The beta quartz develops rapidly as shown by the rapid increase in its diffraction intensity. The diffraction data indicate cell dimensions slightly larger (0.1 Å) than the values in the literature, suggesting the possibility of some stuffing of the lattice.

Beta cristobalite appears abruptly usually at 1100° C. and develops rapidly. The beta quartz phase disappears as the cristobalite develops, indicating a phase inversion. Sample 1 is exceptional in showing the development of cristobalite beginning before 1000° C. and before the

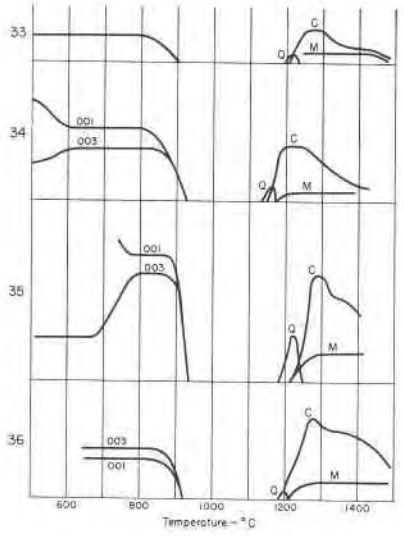

FIG. 6. High temperature phases developed on heating miscellaneous aluminous montmorillonites; Samples 33–36; Q, Beta Quartz; C, Beta Cristobalite; M, Mullite.

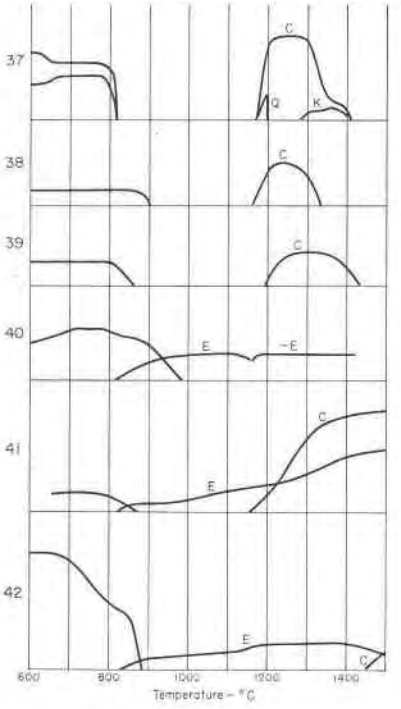

FIG. 7. High temperature phases developed on heating iron-rich montmorillonites (37 and 38), nontronite (39), hectorite (40), saponite (41), and talc (42); Q, Beta Quartz; C, Beta Cristobalite; K, Cordierite; E, Enstatite; C–E, Clinoenstatite.

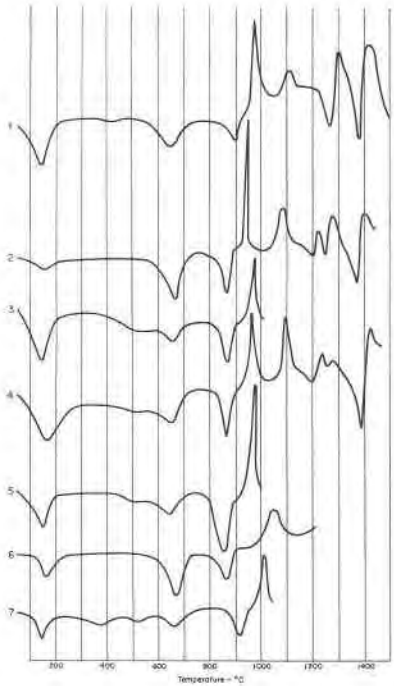

FIG. 8. Differential thermal curves of Cheto-type montmorillonites; Samples 1–7.

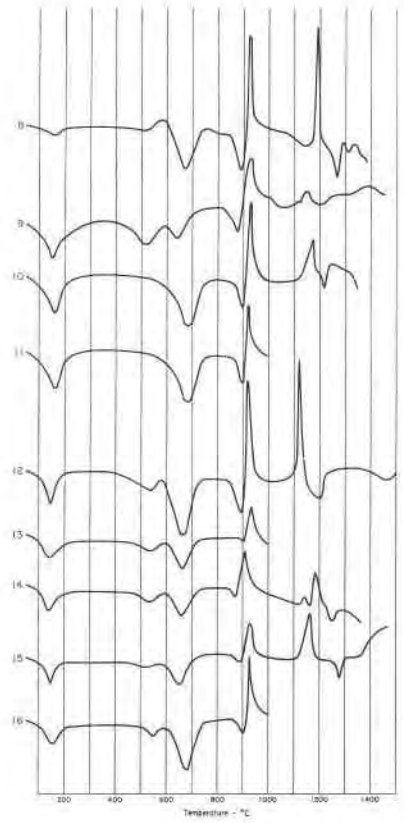

FIG. 9. Differential thermal curves of Wyoming-type montmorillonites; Samples 8–16.

quartz starts to disappear. This same sample also yields a feldspar between about 1000° and 1100° C.

Cordierite appears at 1200°–1300° C. at about the temperature that cristobalite begins to disappear. Its diffraction effects increase in intensity as those of cristobalite decrease.

The samples start to fuse between 1400° and 1500° C. during which interval all of the diffraction effects disappear.

The differential thermal analytical (DTA) curves in Fig. 8 show considerable variation in intensity of the initial endothermic peak due to loss of adsorbed water, but no attempt has been made to study possible causes of this variation. Some samples exhibit a single endothermic reaction between 600° and 700° C. corresponding to the loss of hydroxyl water. Other samples exhibit a double endothermic reaction in the range 450°

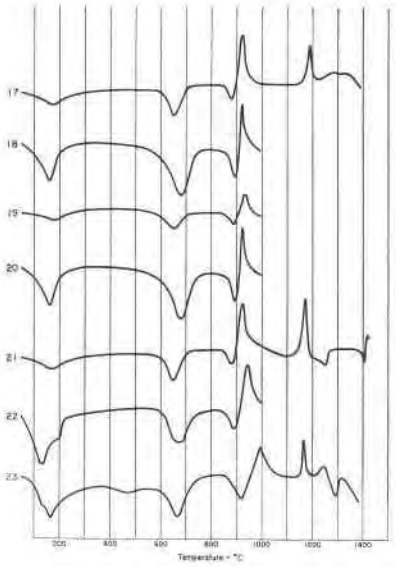

FIG. 10. Differential thermal curves of samples containing Wyoming-type montmorillonite plus free silica; Samples 17–23.

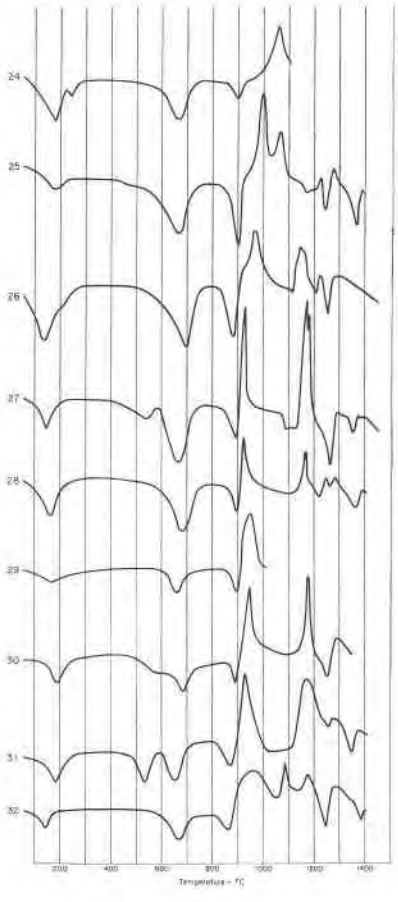

FIG. 11. Differential thermal curves of samples containing a mixture of Chetotype and Wyoming-type montmorillonites; Samples 24–32.

to 700° C. In all cases the endothermic reactions due to loss of hydroxyl water are of slight intensity. A comparison of Figs. 2 and 8 show that the structure of the montmorillonite is not lost with the loss of hydroxyls. It is significant that there is no important change in the *x*-ray diffraction data for the (002) reflections accompanying the loss of hydroxyls.

The DTA curves show a rather intense endothermic reaction between 850 and 900° C., which is the interval in which the structure of the montmorillonite is lost. This endothermic peak is followed after an interval of 50° to 150° C. by a sharp exothermic reaction which can be correlated with the appearance of beta quartz.

A second exothermic reaction appears at about 1100° C. which probably is a consequence of the formation of cristobalite. The DTA curves above about 1200° C. are too complex to be interpreted with certainty.

However, there is a suggestion of an exothermic peak between 1200° and 1300° C. which may correspond to the development of cordierite, an endothermic peak at about 1250° C. probably due to the break up of cristobalite, and another endothermic peak just short of 1400° C. at the temperature of the beginning of the fusion of the samples.

One of the samples (#7) contained cristobalite that could not be separated by fractionation from the montmorillonite. An inspection of the high temperature phase development and the DTA data shows no significant difference from samples of the same type without the excess silica.

Wyoming-Type

Many samples of bentonite from Wyoming are composed of montmorillonite with the characteristics of this type, hence the name.

Figure 3 shows the high temperature phases of samples 8–16 composed of Wyoming-type montmorillonite. The characteristic high temperature phases are cristobalite and mullite. Figure 9 illustrates the DTA data characteristic of this type of montmorillonite.

The montmorillonite on heating in the range of 600° to 700° C. shows generally a decrease in the intensity of the (001) reflection, an increase in the intensity of the (003) reflection and no significant change in the intensity of the (002) reflection.

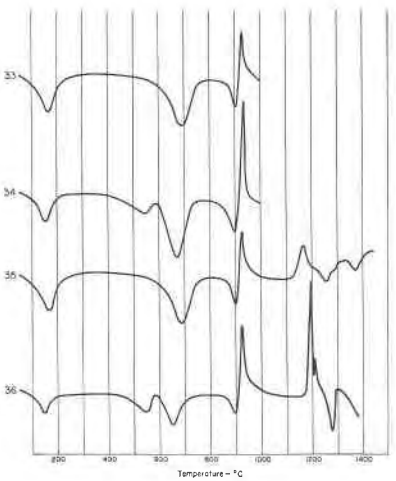

FIG. 12. Differential thermal curves of miscellaneous aluminous montmorillonites; Samples 33-36.

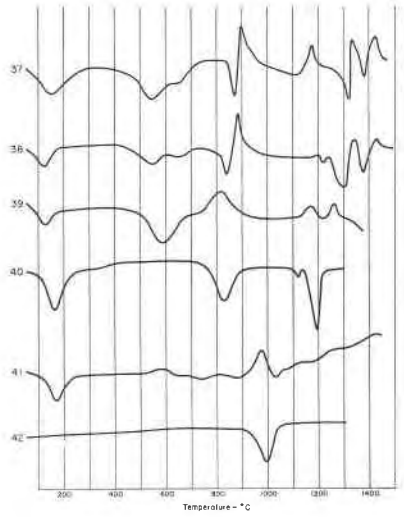

FIG. 13. Differential thermal curves of iron-rich montmorillonite (37 and 38), nontronite (39), hectorite (40), saponite (41) and talc (42).

The montmorillonite structure is lost at 900° to 950° C. and no *x*-ray diffraction effects are noted again for a temperature interval of 200° to 250° C., *i.e.*, until heating is carried to 1100° to 1150° C. at which temperature cristobalite and mullite appear at about the same time. Both of these phases persist until 1400° to 1500° C. when the material fuses. Frequently the cristobalite begins to disappear at about 1300° C. whereas the mullite generally persists unchanged until near the fusion temperature. However, the intensity of the mullite reflections is never very great indicating that this phase is never very abundant and/or very well crystallized. The lattice dimensions of the mullite vary slightly from published values for the pure mineral suggesting some replacements or defects.

The characteristics of the initial endothermic peaks on the DTA curves will not be considered herein. The curves all show a fairly intense endothermic reaction between 600° and 700° C. due to the loss of hydroxyl water. Some of the samples show another endothermic peak between 500° and 600° C. making a dual peak for the dehydroxylations. In general these dehydroxylation endothermic peaks are more intense for the Wyoming-type than for the Cheto-type montmorillonites. The *x*-ray data show that the structure of the montmorillonite persists through the loss of hydroxyls but that some structural changes take place which are adequate to cause changes in the relative intensities of the basal spacings. The DTA curves show an endothermic reaction of variable intensity at about 900° C., which is the temperature at which the diffraction effects from montmorillonite disappear. This endothermic peak is followed immediately by an exothermic reaction and it is of special interest that there is no crystalline phase shown at this temperature by the *x*-ray diffraction data, *i.e.*, this thermal reaction occurs at a temperature interval in which there are no *x*-ray reflections.

The DTA curve shows an exothermic reaction (sometimes more than one) at 1100° to 1200°C. which is the temperature at which mullite and cristobalite appear. The DTA curves beyond this temperature are quite irregular and variable, and cannot be interpreted.

Wyoming-Type With Excess Silica

Many of the samples containing the Wyoming-type montmorillonite also had quartz and/or cristobalite in small amounts (less than 15%) in particles so small that they could not be separated by fractionation from the montmorillonite. It is interesting that only one sample (#7) of Cheto-type montmorillonite was found with such free silica. The results of the high temperature diffraction studies of the Wyoming type samples with excess silica (numbers 17–23) are given in Fig. 4. DTA curves for the

same samples are given in Fig. 10. The diffraction effects of the quartz are not shown in Figure 4 since they did not influence the high temperature phase development.

A comparison of Figs. 3 and 4 show that the excess silica had no detectable effect on the development of high temperature phases. A comparison of the DTA curves in Figs. 9 and 10 show no large differences. The thermal reactions, especially the exothermic ones, are usually relatively less intense in the samples with excess silica. Also it is interesting, although the possible significance is not presently known, that none of the samples with excess silica show a double peak for the loss of hydroxyl water.

Mixtures of Cheto- and Wyoming-Types

Figure 5 shows high temperature phase data for samples (numbers 24–32) which exhibit characteristics of both of the Cheto- and Wyoming-types. Samples 27, 28 and 30 show cristobalite and mullite which are characteristic of the Wyoming-type plus cordierite which is characteristic of the Cheto-type. The DTA curves, Figure 11, of these same samples are like those of the Wyoming type and it seems likely that the dominant component of these samples is Wyoming-type montmorillonite.

Samples 24, 25, 26 and 29 show beta quartz and cristobalite high temperature phases like those of the Cheto-type plus mullite. In samples 24 and 26 cordierite has not developed. These samples except #29 show DTA curves characteristic of the Cheto-type montmorillonite and it seems likely that this type is dominant in these samples. The DTA curve of sample 29 resembles more those of the Wyoming-type than the Cheto-type, however, the first exothermic peak is unusually broad and could well be interpreted as a composite of the peaks in the Wyoming- and Cheto-types. The suggested interpretation is that sample 29 contains roughly equal amounts of Cheto- and Wyoming-type montmorillonites.

It is of interest that the sample investigated from the type locality at Montmorillon, France (#31) is a mixture of the Cheto- and Wyoming-types.

Sample 32 is composed of a mixture of the montmorillonite types plus cristobalite which could not be separated by fractionation. The high temperature phase development shows nothing unique. The exothermic reaction at about 900° C. seems unusually broad and may again be interpreted as due to the mixing of about equal parts of the two types of montmorillonite.

It is recognized that another possible interpretation is that these data do not indicate mixtures of two types of montmorillonite, but rather variations in the composition within a single type. It will be shown pres-

ently that there is strong additional evidence for mixing of types, although there is undoubtedly some variation in composition within each type.

Miscellaneous Samples

It is not meant to imply that all aluminous montmorillonites belong to the two classes indicated above. Figures 6 and 12 present high temperature phase and DTA data for samples that do not fit exactly in either of these two categories. Thus samples 33, 34, 35 and 36 have DTA curves like those of the Wyoming-type, and the high temperature phase characteristics are also like those of the Wyoming-type except for the small amount of quartz forming just prior to the development of cristobalite. It is expected therefore, that these samples would not differ in any very substantial way from those of the Wyoming type. A possible explanation for the presence of the beta quartz phase will be presented later in the Discussion.

Figures 7 and 13 present high temperature phase DTA data for a few montmorillonites with a high iron content (37, 38), a sample of nontronite (39), samples with a high magnesium content (40, 41), and a sample of talc (42). Samples with increasing replacements of aluminum by iron (samples 37, 38 and 39), show the absence of mullite at high temperatures. In samples with abundant iron (38, 39), cristobalite is the only high temperature phase. The destruction of the montmorillonite lattice tends to be at lower temperatures (800° to 900° C.) in the iron-rich samples as compared to the aluminous types. Also the cristobalite disappears finally at a slightly lower temperature in the iron-rich montmorillonites. The DTA curves for these high iron samples show a lower temperature for the endothermic dehydroxylation peaks than is the case for the aluminous types. Also the endothermic peak for the loss of structure is at a relatively lower temperature in the iron-rich types. In the nontronite sample (39) there is no peak accompanying the loss of structure, perhaps because of a gradual destruction of the structure which is in accordance with the *x*-ray data shown in Fig. 7. The DTA curves for the iron-rich samples show an exothermic reaction between 800° and 900° C. which is not accompanied by any crystalline phase detectable by *x*-ray diffraction. No definite explanation can be offered, but it is the authors' opinion that it represents the nucleation of a phase with a silica type crystallization. The slight second exothermic reaction just short of 1200° C. is at the temperature at which cristobalite appears in high temperature diffraction data. The DTA curves above 1200° C. are to complex to be interpreted.

In the case of hectorite (40) the structure is lost gradually from about 800° C. to 1000° C. Enstatite appears as soon as the structure of hector-

ite begins to disappear and the maximum diffraction of enstatite is attained while the hectorite is still producing considerable diffraction intensity. At about 1125° C. enstatite changes to clinoenstatite. No other high temperature phases were evident. The endothermic reactions at about 800° C. and 1200° C. are in the range of the loss of montmorillonite structure and the formation of enstatite, and the inversion of the enstatite to clinoenstatite, respectively. The saponite sample (41) loses its structure from about 800° C. to 875° C. without a corresponding DTA peak in accordance with its trioctahedal structure. Enstatite begins to form at a slightly lower temperature than that of the final loss of the saponite structure with no corresponding DTA peak. The intensity of the enstatite diffraction continues to increase to the highest temperature attained, 1500° C. Cristobalite begins to form at about 1150° C. and the intensity of its diffraction effects also continue to increase to the highest temperature attained. The DTA curve for saponite shows only one moderately intense thermal reaction, the exothermic reaction at about 975° C., and no definite correlation is possible between the DTA curve and the high temperature phase data.

The talc sample (42) loses its structure between about 700° C. and 880° C. Enstatite appears at a slightly lower temperature than that of the final loss of the talc structure and continues to diffract with moderate intensity up to the highest temperature attained, 1500° C. Cristobalite appears first at 1450° C. with very minor diffracting intensity which is, however, increasing at 1500° C. The DTA curve for talc shows a single thermal reaction, an endothermic one just short of 1000° C., which cannot be correlated with any of the high temperature phase reactions.

Chemical Analyses

Chemical analyses of all samples together with structural formulae computations according to the method of Ross and Hendricks (1944) are given in Tables 2 to 6.

The computed compositions of octahedral cations for all the montmorillonite samples are plotted in Fig. 14.

The chemical compositions of the aluminous samples fall into two groups corresponding to those derived from the high temperature diffraction and DTA data. The samples classed as Cheto-type, Table 2, have less than 5% of tetrahedral silicon replaced by aluminum; 25 to 35% of octahedral aluminum replaced by magnesium; and 5% or less of the octahedral positions populated by iron.

In general the Wyoming-type montmorillonites, Table 3, show about the same amount of the tetrahedral silicon replaced by aluminum, although in some samples the amount of tetrahedral aluminum is greater

TABLE 2. CHEMICAL ANALYSES OF CHETO-TYPE MONTMORILLONITES

Sample Number	SiO_2	Al_2O_3	TiO_2	Fe_2O_3	FeO	MgO	CaO	Na_2O	K_2O	H_2O+	H_2O+ 105–500	H_2O+ 500–900	H_2O-	Si	Al. Tet.	Al. Oct.	Fe″	Fe‴	Mg	Total Oct.
1	61.77	19.85	.24	1.95*		5.56	1.89	.07	.09	7.72			9.49	3.91	.09	1.38		.09	.54	2.01
2	62.23	21.03		1.75	.48	5.70	0	.65	0		4.45	2.93	8.41	3.86	.14	1.39	.02	.08	.55	2.04
3	63.07	18.46	.28	1.99*		7.38	.24	.16	.16	7.17			13.03	3.93	.07	1.28		.09	.71	2.08
4	61.55	20.44		2.02	.38	6.06	0	.30	0		5.84	2.45	7.67	3.84	.16	1.34	.02	.09	.58	2.03
5	60.90	20.71		2.06	.36	6.84	.30	.23	0		5.99	2.03	7.08	3.81	.19	1.33	.02	.09	.65	2.09
6†	60.80	22.15		.07		4.44	3.74			8.71			14.75	3.98	.02	1.67			.38	2.05
7	65.97	19.10		1.09	.76	4.56	0	.13	0		4.80	2.40	5.49	‡		1.46	.03	.05	.46	

Analyses based on dry (105° C.) weight of samples.
* Total Fe as Fe_2O_3.
† Crude clay.
‡ Contains free silica.

TABLE 3. CHEMICAL ANALYSES OF WYOMING-TYPE MONTMORILLONITES

Sample Number	SiO_2	Al_2O_3	TiO_2	Fe_2O_3	FeO	MgO	CaO	Na_2O	K_2O	H_2O+	H_2O+ 105–500	H_2O+ 500–900	H_2O-	Si	Al. Tet.	Al. Oct.	Fe″	Fe‴	Mg	Total Oct.
8	64.80	24.54		1.27	.56	1.60	0	.40	0		2.84	3.87	6.22	3.96	.04	1.72	.03	.06	.15	1.96
9	62.00	23.42		3.74	.32	.93	.68	.72	2.63		3.86	1.35	6.44	3.92	.08	1.66	.02	.18	.09	1.95
10	62.30	23.50		3.35	.37	1.95	.31	.40	.03		2.01	4.44	7.81	3.90	.10	1.64	.02	.15	.19	2.00
11	62.70	22.20		4.62	.48	2.00	.58	.01	.12		2.44	4.62	7.13	3.92	.08	1.55	.03	.22	.19	1.99
12	59.73	24.30		5.54	.37	2.10	0	.80	.22		3.88	2.71	13.70	3.76	.24	1.56	.02	.26	.20	2.04
13	60.22	23.67	.34	6.28*		1.46	.13	.09	.19	6.86			6.81	3.80	.20	1.56		.30	.14	2.00
14	60.76	23.08	.38	6.10*		1.44	.17	.13	.21	6.07			7.65	3.84	.16	1.56		.29	.14	1.99
15	59.91	21.97	.33	6.72*		2.15	.34	.09	.11	6.66			8.81	3.83	.17	1.48		.32	.21	2.01
16	58.67	27.34		3.64	.38	2.00	0	.62	.18		3.22	3.82	10.88	3.66	.34	1.67	.01	.17	.19	2.05

Analyses based on dry (105° C.) weight of samples.
* Total Fe as Fe_2O_3.

than is the Cheto-type samples. In the Wyoming-type montmorillonite 5 to 10% of the octahedral aluminum is replaced by magnesium (less than for the Cheto-type); and 5 to more than 15% of the octahedral positions are populated by iron which is more than for the Cheto-type. The total octahedral population is generally 2 or slightly less in the Wyoming-type samples, whereas for the Cheto-type this value is generally slightly greater than 2.

The analyses of the Wyoming-type sample containing free silica show, Table 4, the expected relatively large amount of SiO_2.

Samples composed of mixtures of Cheto-and Wyoming-type montmorillonites have chemical compositions, Table 5, that are intermediate between the pure Wyoming- and Cheto-types.

Samples 33, 34, 35 and 36, which differ from the Wyoming-type samples because a small amount of beta quartz formed as an initial high temperature phase, and which are listed among the Miscellaneous samples in Table 6, have chemical compositions similar to those of the Wyoming-type samples, Fig. 14.

Samples 37 and 38, Table 6, show some characteristics of both the Cheto- and Wyoming types in the larger replacement of octahedral

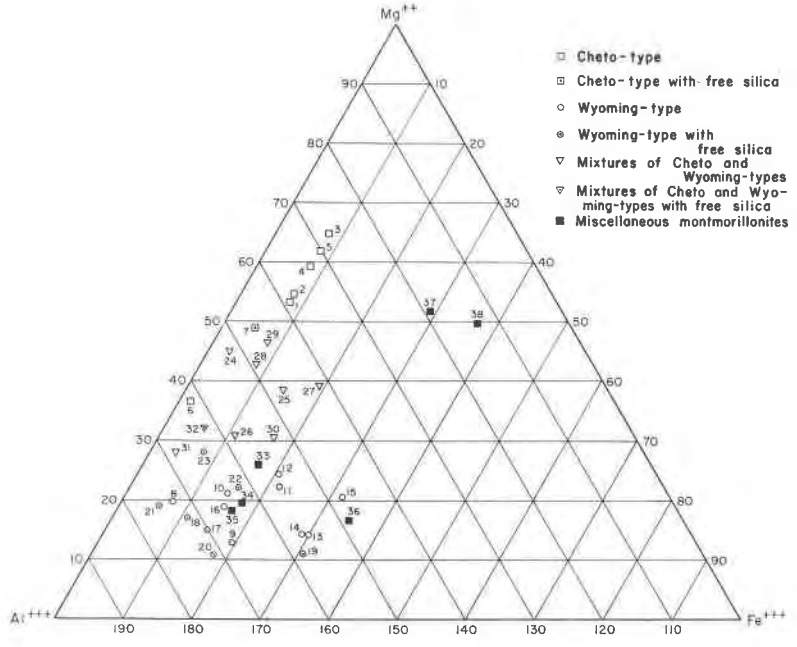

FIG. 14. Computed octahedral cation compositions of the montmorillonites.

TABLE 4. CHEMICAL ANALYSES OF WYOMING-TYPE MONTMORILLONITE CONTAINING ALSO QUARTZ AND/OR CRISTOBALITE

Sample Number	SiO_2	Al_2O_3	Fe_2O_3	FeO	MgO	CaO	Na_2O	K_2O	H_2O+ 105–500	H_2O+ 500–900	H_2O-
17	68.60	19.00	2.66	.45	1.07	2.52	.49	0	2.10	4.33	5.08
18	67.50	22.60	2.32	.35	1.41	.34	.09	.07	2.47	4.31	5.04
19	63.00	19.90	6.02	.57	.75	1.55	.40	.24	3.19	3.66	7.28
20	66.74	20.54	3.39	.38	.79	.42	.78	0	2.94	3.41	7.13
21	66.90	22.98	1.29	.28	1.76	0	.52	.01	3.61	2.51	5.34
22	66.26	20.49	3.25	.48	1.88	.45	.26	.03	3.78	2.55	10.26
23	72.45	17.52	1.45	.49	2.16	0	.10	0	2.58	2.97	7.57

Analyses based on dry (105° C.) weight of samples.

TABLE 5. CHEMICAL ANALYSES OF MIXTURES OF CHETO- AND WYOMING-TYPE MONTMORILLONITES

Sample Number	SiO_2	Al_2O_3	TiO_2	Fe_2O_3	FeO	MgO	CaO	Na_2O	K_2O	H_2O+	H_2O+ 105–500	H_2O+ 500–900	H_2O-	Si	Al. Tet.	Al. Oct.	Fe''	Fe'''	Mg	Total Oct.
24	61.63	24.92		.70	.78	4.51	0	.37	0		3.38	3.65	12.68	3.77	.23	1.56	.04	.03	.42	2.05
25	65.00	22.80		3.07	.40	3.90	.05	.17	.13		2.36	4.22	12.10	3.87	.13	1.47	.02	.14	.36	1.99
26	61.40	25.03		2.52	.23	3.26	.33	.62	0		3.06	3.76	11.03	3.78	.22	1.59	.01	.12	.31	2.03
27	60.70	20.28	.39	4.07*		3.98	.75	.62	.17	7.66			8.27	3.90	.10	1.43		.20	.39	2.02
28	61.56	22.99	.04	2.23*		4.48	.30	.12	.17	7.05			7.13	3.85	.15	1.51		.10	.43	2.04
29	60.62	22.18	.40	2.06*		4.80	.38	.06	.03	8.31			9.07	3.83	.17	1.48		.10	.49	2.07
30	63.37	23.37		3.82	.47	3.22	0	.63	0		3.35	2.67	7.80	3.91	.09	1.53	.02	.18	.30	2.03
31†	60.16	23.24		.98		3.79	1.91	.04	.13	9.39			14.81	3.97	.03	1.73		.05	.36	2.14
32	69.58	19.41		1.34	.75	2.57	0	.29	0		2.92	2.99	8.47	‡		1.62	.04	.06	.28	

Analyses based on dry (105° C.) weight of samples.
* Total Fe as Fe_2O_3.
† Crude clay.
‡ Contains free silica.

TABLE 6. CHEMICAL ANALYSES OF MISCELLANEOUS SAMPLES

Sample Number	SiO_2	Al_2O_3	TiO_2	Fe_2O_3	FeO	MgO	CaO	Na_2O	K_2O	H_2O+	H_2O+ 105–500	H_2O+ 500–900	H_2O-	Si	Al. Tet.	Al. Oct.	Fe''	Fe'''	Mg	Total Oct.
33	62.75	22.12	.15	3.94*		2.64	.29	.20	.06	6.70			8.96	3.94	.06	1.57		.17	.26	2.00
34	59.01	27.17		3.78	.27	2.20	0	.28	.22		3.96	3.13	8.44	3.70	.30	1.66	.01	.18	.21	2.06
35	60.20	26.20		3.76	.34	1.92	.04	.34	.02		2.31	4.58	7.05	3.75	.25	1.67	.02	.17	.18	2.04
36	60.00	19.70		6.70	.56	1.33	2.60	.53	.06		4.28	2.94	8.24	3.95	.05	1.48	.03	.33	.13	1.97
37	59.98	18.69	.20	6.47*		5.44	.22	.03	.30	7.99			7.77	3.81	.19	1.21		.31	.53	2.05
38	56.28	19.51		9.20	.23	4.95	0	.94	.92		5.32	2.22	11.80	3.65	.35	1.14	.01	.45	.49	2.09
39	50.10	3.75		34.87	.75	.63	.26	.14	.05		6.34	1.85	14.20							
40†	59.76	.15		.03		28.68	.18	3.37	.26	6.21	$Li_2O=1.35$		9.29	3.98	.02		Li=.35		2.81	3.61
41†	55.00	1.20		1.40		28.00	.01	—	.52		10.33			3.96	.04	.06		.07	2.92	3.05

Analyses based on dry (105° C.) weight of samples.
* Total Fe as Fe_2O_3.
† Crude clay.

aluminum by magnesium of the former and the relatively large replacement of tetrahedral silicon by aluminum of the latter. In addition these samples have a larger amount of iron than the Cheto- and Wyoming-type samples.

The sample of nontronite (39) has only a small amount of replacement of magnesium for iron in octahedral positions. The nontronite sample as well as the samples with considerable replacement of the aluminum by iron in octahedral positions (37 and 38) are dioctahedral forms, but the total population of octahedral positions is appreciably in excess of 2.

The samples of hectorite (40) and saponite (41) both are trioctahedral forms in which magnesium is the dominant component of the octahedral layer. It is interesting in both of these samples the tetrahedral layers have very little replacement of silicon by aluminum and in each case the total population of octahedral positions is slightly in excess of 3.

Cation Exchange Capacity

The cation exchange capacities of the samples determined and computed are listed in Table 7. The determined capacities of the Cheto-type montmorillonite ranges between 114 and 133 milliequivalents per 100

Table 7. Cation Exchange Capacity in Milliequivalents per 100 Grams

Sample No.	Determined	Computed	Sample No.	Determined	Computed
	Cheto-type			Mixture of Cheto- and Wyoming-types	
1	133	168			
2	114	160	25	113	151
3	118	151	26	114	126
4	125	182	27	114	126
5	125	161	28	118	129
6	122		29	110	126
			30	109	90
			30	103	
	Wyoming-type		32	57	(contains free silica)
8	109	95		Miscellaneous Samples	
9	91	95			
10	89	87	33	106	90
11	98	92	34	90	95
12	96	106	35	117	92
13	111	95	36	106	89
14	110	92	38	93	160
15	109	98	39	88	160
16	102	123	40	82	

gram, whereas the capacities of the Wyoming-type samples ranges from 89 to 111 milliequivalents per 100 gram. It is interesting that there is no overlap in the capacities between these types of montmorillonites.

The relatively higher exchange capacity of the Cheto-type is in agreement with a greater total replacement and higher net negative charge on the lattice of this type of montmorillonite as compared to the Wyoming-type. In the Wyoming-type most of the charge is derived from replacements in tetrahedral positions, but the total charge on the lattice is less than for the Cheto-type montmorillonite.

The samples which are mixtures of the two types have cation exchange capacities, which are intermediate as would be expected.

The miscellaneous samples with the exception of #35 have capacities similar to those of the Wyoming-type montmorillonite. The aluminous samples in this miscellaneous group (nos. 33, 34, 35 and 36) also have chemical compositions which are quite similar to those of the Wyoming-type. Miscellaneous samples 38, 39 and 40 are high iron or magnesium montmorillonite samples and data are not at hand to indicate whether or not these values have any general significance.

For the Wyoming-type montmorillonite, there is reasonable agreement between the determined and the computed cation exchange capacities. However, for the Cheto-type, the computed values are uniformly higher than the determined values by the order of about 35 milliequivalents per 100 grams. The only explanation that can be offered for this lack of agreement in the Cheto-type is that it is a consequence of the preparation of the samples. The samples for chemical analyses were prepared using acid, whereas for the exchange capacity determinations the samples were untreated. Perhaps the acid treatment removed some cations from within the lattice thereby increasing the computed value. If this is the explanation, it follows that the Cheto-type is more susceptible to leaching than the Wyoming-type montmorillonite.

In the case of mixtures, the computed values are in general higher than the determined values in accord with the presence of some Cheto-type material.

The foregoing explanation is supported by the much higher computed values for the iron rich samples (38, 39) as compared to the determined values. It would be expected that the lattice iron would be relatively more affected by the acid treatment.

X-Ray Diffraction of Unfired Samples

Powder Diagrams

The diagrams for the Cheto-type montmorillonites as compared to the Wyoming-type show somewhat better defined prism reflections, the (001)

reflections are frequently sharper, and there is a more definite indication of higher basal orders.

In the case of mixtures of the two types of montmorillonite, the prism reflections are like those of the Wyoming type. The (001) reflections are variable with similarities to both types represented in different samples.

The sample listed as containing free silica shows diffraction lines for cristobalite and/or quartz in addition to those from montmorillonite. Except for the expected reduction in intensity of the montmorillonite reflections, there is no significant difference in the patterns of these samples as compared to those with little or no free silica.

TABLE 8. COMPUTED AND MEASURED VALUES FOR b

Sample No.	Computed	Measured	Sample No.	Computed	Measured
Cheto type			Wyoming type (*cont.*)		
1	8.966	9.00	13	8.972	8.97
2	8.973	9.01	14	8.966	8.97
3	8.981	8.98	15	8.975	8.97
4	8.979	8.97	16	8.98	8.97
5	8.987	9.00	Miscella-		
6	8.938	8.95	neous types		
Wyoming type			33	8.951	8.95
8	8.933	8.965	34	8.978	8.965
9	8.944	8.94	35	8.97	8.98
10	8.95	8.97	36	8.958	8.97
11	8.956		37	8.998	9.00
12	8.979	8.97	38	9.03	9.04

Miscellaneous samples (33, 34, 35, 36) give diffraction data like those of the Wyoming-type. Sample 38 with a higher iron content is also like that of the Wyoming type. The sample of nontronite gives poorer data than the Wyoming-type in that the prism reflections are merely broad bands.

The values of b_0 determined from the (060) reflections observed on the powder diagrams and calculated according to the formula of MacEwan (1951) for the Wyoming, Cheto, and miscellaneous types are given in Table 8. All specimens appear to be dioctahedral montmorillonites. The agreement between the observed and computed values is reasonably good. The Wyoming-type samples observed values range from 8.94 to 8.97. The miscellaneous samples (33, 34, 35, 36) range from 8.95 to 8.98. The values for the Cheto type range from 8.97 to 9.01—higher than the

Wyoming type as would be expected because of the higher content of magnesium. An exception in the case of the Cheto-type is the Tatatilla sample (6) for which the value is unusually low probably because of the extremely small iron content. The values for the samples with a high iron content (37, 38) are 9.00 to 9.04 which is in the expected range. The

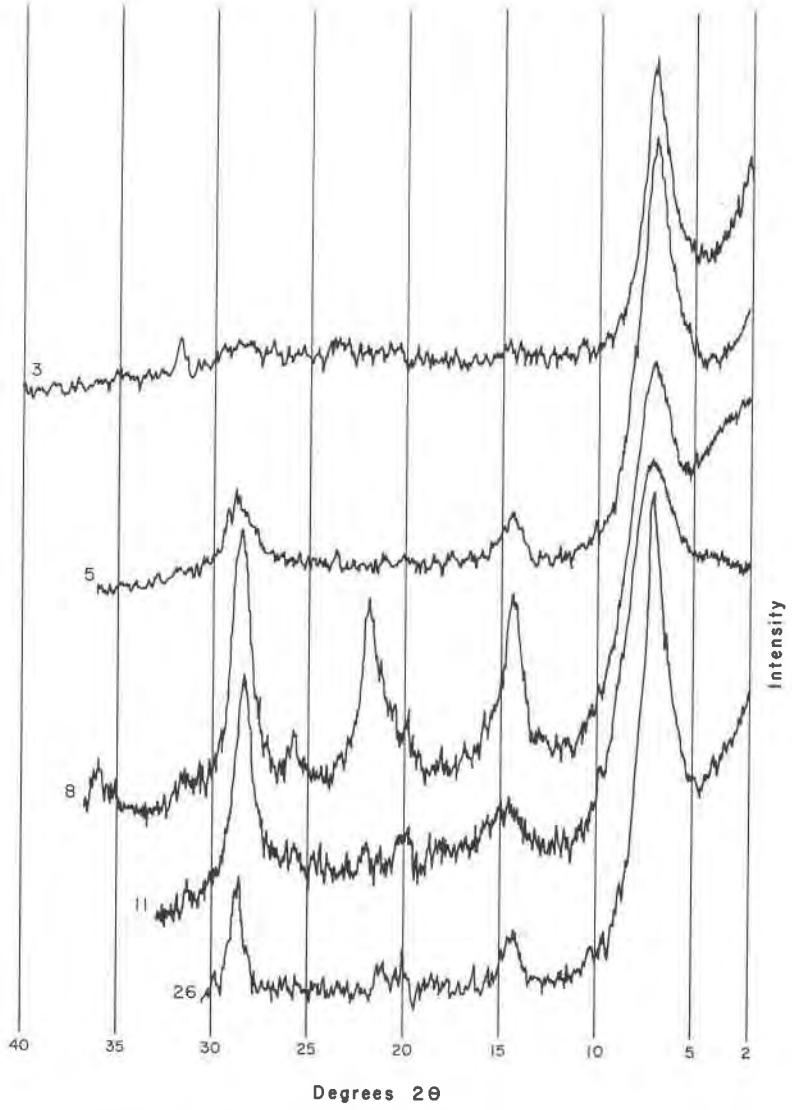

Fig. 15. *X*-ray diffraction spectrograms of oriented aggregates of Cheto-type montmorillonite (3 and 5), Wyoming-type montmorillonite (8 and 11), and a mixture of these types (26).

(060) reflection for most of the samples is fairly sharp but for others it is fairly broad, sometimes suggesting that it is a complex of several reflections. The samples composed of a single type of montmorillonite are in general sharper than those composed of mixtures. This is true for all of the Cheto-type samples but not for all of the Wyoming-type samples. Further, a few of the samples composed of mixtures yield quite sharp (060) reflections. It may be concluded from the foregoing statements that powder diffraction data may suggest that a given sample is composed of a particular type of montmorillonite or a mixture, but it is no more than a suggestion. The data seem to indicate that the population of cation positions in a mass of montmorillonite is more uniform in the Cheto-type than in the Wyoming-type mineral.

Oriented Aggregate Diagrams

The Cheto-type samples show intense sharp (001) reflections but higher orders are always of about uniform low intensity both with and without glycol treatment, Figs. 15 and 16. On the other hand, the Wyoming-type samples usually show sharp (001) reflections and also sharp intense higher orders up to about (006). The sharp higher orders were obtained from one sample without glycol treatment, but for the other samples glycol treatment was necessary to develop them.

The samples containing excess silica were substantially like those of the purer montmorillonites. The Wyoming-type with excess silica show the same sharp higher orders up to about (006) as those without the silica, indicating that the quartz or cristobalite is present in discrete particles even though it has been impossible to separate it from the montmorillonite.

The samples composed of mixtures, following glycol treatment, show the sharp higher orders like the Wyoming-type except that they are somewhat less intense. The (004) and (006) reflections are relatively weaker than the (002), (003), and (005) reflections and this characteristic is more pronounced in the mixtures than in the pure Wyoming-type mineral.

The miscellaneous samples of the aluminous montmorillonites show the development of higher orders comparable to the Wyoming type. The nontronite sample also shows the development of higher orders, but as would be expected the relative intensities are different from those of the aluminous samples.

It is planned to consider further the diffraction characteristics of these types of montmorillonite in a later paper. It appears, however, that the data warrant the conclusion that the Wyoming-type is composed of unit silicate layers less well bonded together than the Cheto-type, so that the montmorillonite can be more completely dispersed leading to more uni-

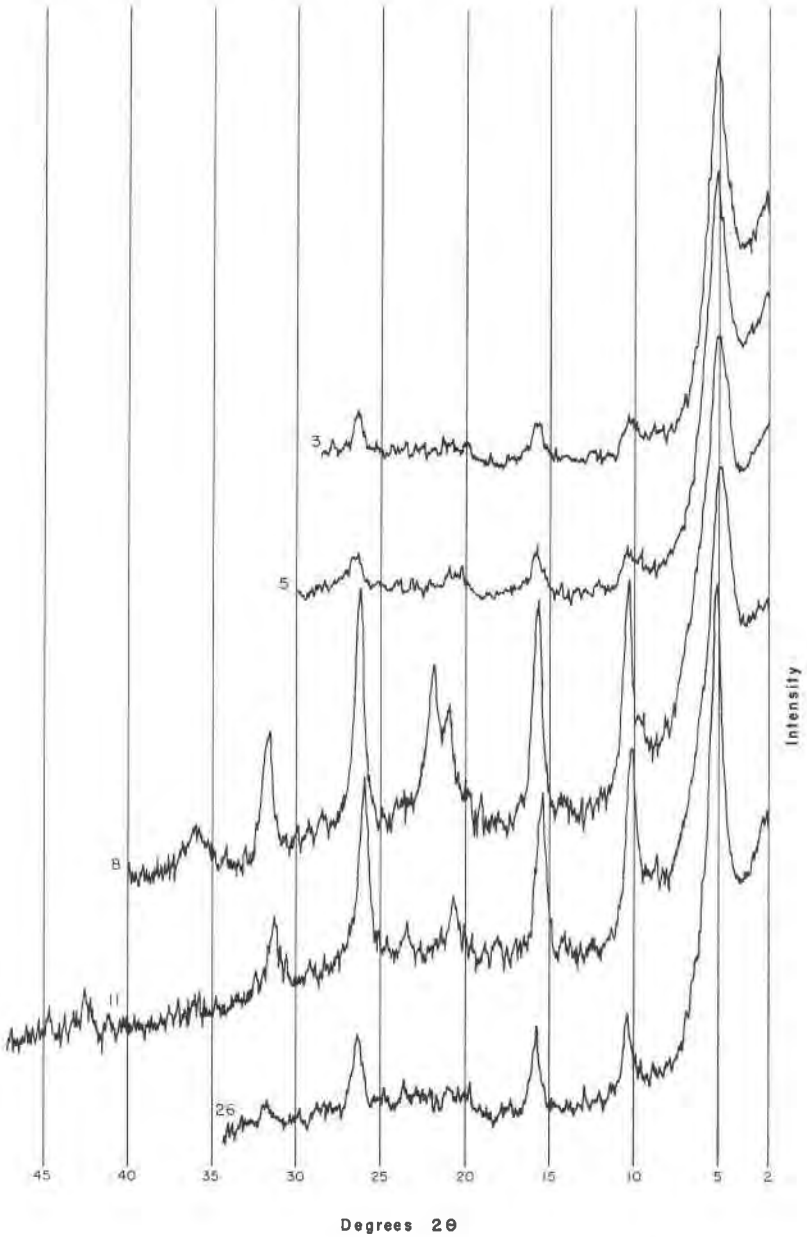

FIG. 16. *X*-ray diffraction spectrograms of oriented aggregates, glycol treated, of Cheto-type montmorillonite (3 and 5), Wyoming-type montmorillonite (8 and 11), and a mixture of these types (26).

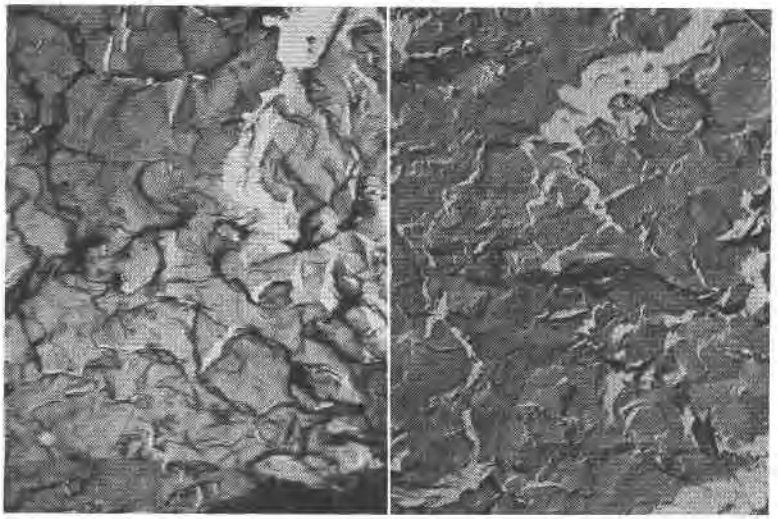

FIG. 17. Electron micrographs (carbon replicas) of Wyoming-type montmorillonite (10), 6500×.

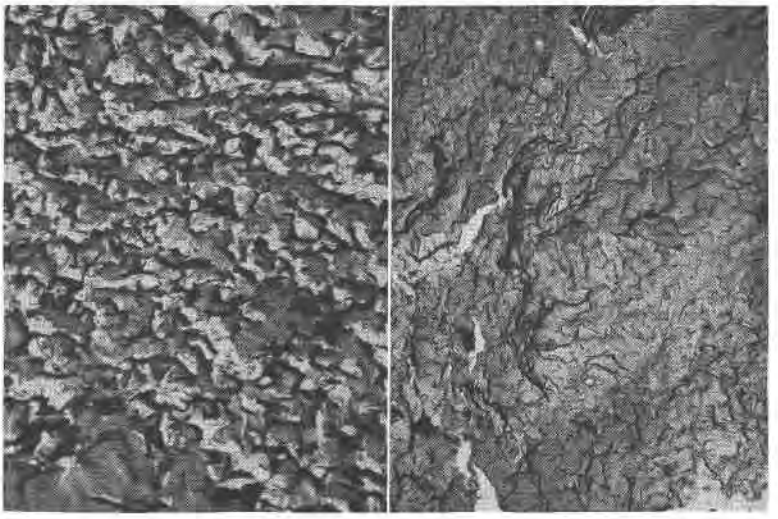

FIG. 18. Electron micrographs (carbon replicas) of Cheto-type montmorillonite (6), 6500×.

formly oriented aggregate flakes which are more thoroughly and completely penetratable by the glycol. This is in accord with the relatively low cation exchange capacity and hence lower charge on the lattice of the Wyoming type which in turn is the consequence of a relatively smaller amount of substitution within the lattice of the Wyoming-type montmorillonite.

Electron Diffraction and Microscopy

The electron diffraction and microscopic characteristics of the samples were not investigated exhaustibly but only to determine if there were obvious differences corresponding to the Wyoming- and Cheto-types of montmorillonite. No such differences could be found in the diffraction data.

Electron micrographs using the carbon replica technique indicate that the Wyoming type, Fig. 17, is composed of such extremely small particles that there is no suggestion of individual particles in the micrographs. On the other hand, micrographs of the Cheto-type, Fig. 18 and the sample from Montmorillon, Fig. 19, which is a mixture of types, have a granular appearance suggesting somewhat coarser particles. It is not felt that the electron micrographs present unequivocal evidence for separating the two types. However, the characteristics of the electron micrographs are gen-

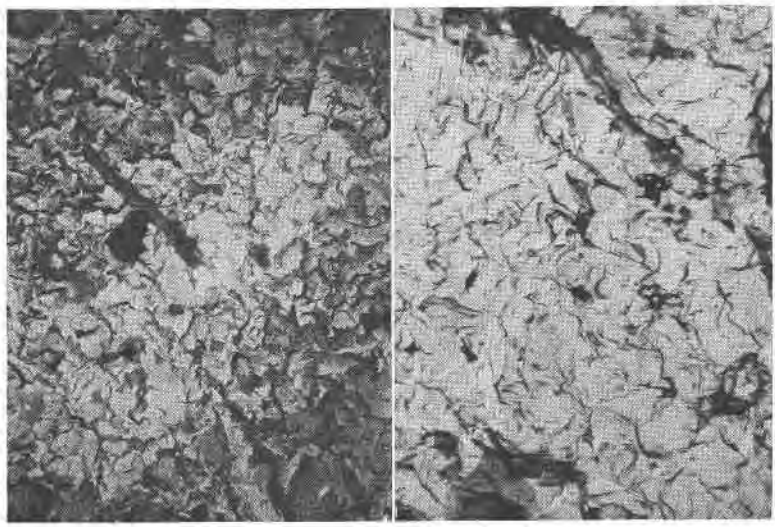

Fig. 19. Electron micrographs (carbon replicas) of samples composed of mixture of Wyoming- and Cheto-type montmorillonite, (31), 6500×.

erally in accord with the characteristics of the two types of aluminous montmorillonite derived from the other data.

Electron micrographs of the same samples after heating to a temperature just adequate to destroy the montmorillonite structure (900° C.±) showed no significant differences as compared to the unfired samples.

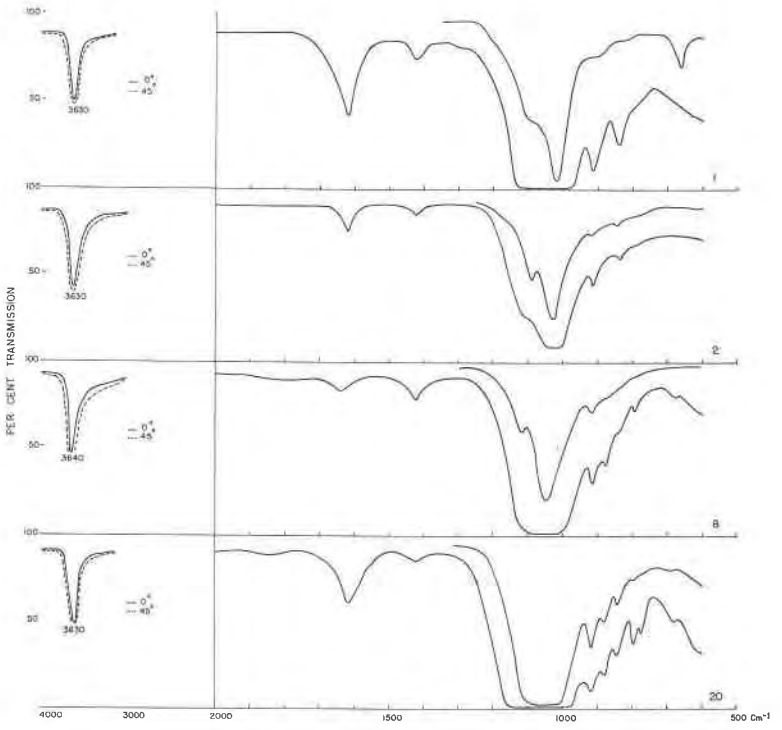

FIG. 20. Infra-red absorption curves of montmorillonites: Cheto-type (1 and 2), Wyoming-type (8), Wyoming-type plus quartz (20). All data from films except separate curves 600–1300 cm^{-1} from KBr pellets.

INFRA-RED ANALYSES

Infra-red absorption curves were obtained for a series of samples showing differences in chemical composition, *x*-ray diffraction, and DTA characteristics by Dr. J. M. Serratosa of the Illinois State Geological Survey. The authors are indebted to Dr. Serratosa for the interpretation of the infra-red data which are presented in Figs. 20 to 23.

Films composed of particles with parallel orientation of the basal cleavage planes were prepared by evaporating a suspension on plastic slides; when dried the films are easily separated with ethyl alcohol. These

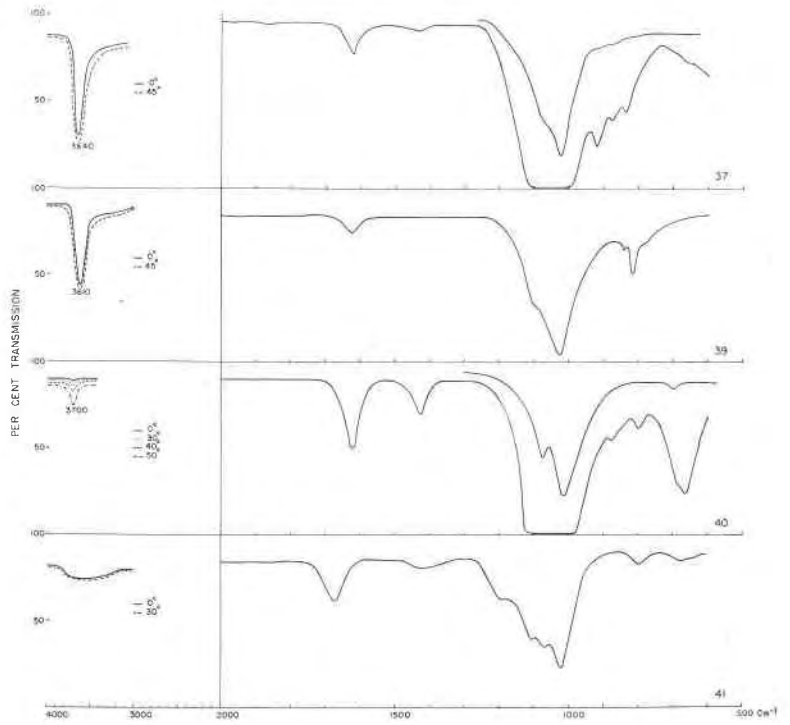

FIG. 21. Infra-red absorption curves of iron-rich montmorillonite (37), nontronite (39), hectorite (40), and saponite (41). All data from films except separate curves 600–1300 cm^{-1} from KBr pellets.

films were heated to 300° C. and protected with fluorolube oil in order to avoid rehydration. Infra-red spectra were obtained for different incident angles. Serratosa and Bradley (1958) have shown that among micas and related crystallizations trioctahedral compositions exhibit an OH bond axis normal to the cleavage flake with an infra-red absorption frequency near 3700 $cm.^{-1}$, but that the dioctahedral compositions exhibit OH bond axes near the plane of the cleavage flake and of lesser absorption frequency. Determination of the direction of the OH bond axis by obtained spectra of oriented aggregates for different incident angles therefore provides a means of identifying the dioctahedral or trioctahedral nature of such crystallization.

In the 3700 $cm.^{-1}$ region all of the samples of montmorillonite and nontronite examined showed a strong absorption for normal incidence with little sensitivity to the orientation of the flake, thereby indicating that the crystallization in these samples is dioctahedral. It must be noted that it is uncertain whether a mixture of dioctahedral and trioctahedral forms

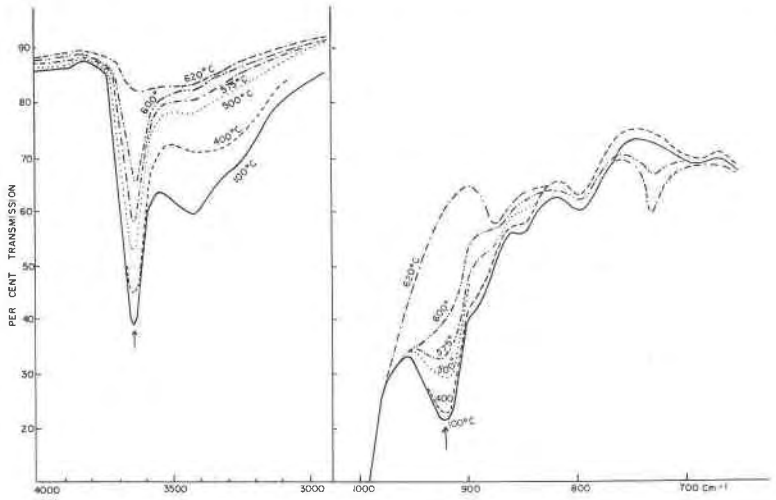

FIG. 22. Infra-red absorption curves of sample 27 composed of a mixture of Cheto- and Wyoming-type montmorillonite, and after heating to temperatures indicated.

could be detected with the equipment used (NaCl prism), if one of the components was present in small amounts. There is therefore, the possibility that a small amount of trioctahedral material may be present in these samples. It is of interest that the maximum absorption of the montmorillonites corresponds to that of muscovite (3640 cm.$^{-1}$), whereas that of the nontronites, is lower (3600–3610 cm.$^{-1}$).

The samples of saponite and hectorite, Fig. 21, show an absorption at higher frequencies (3700–3710 cm.$^{-1}$) which increases markedly with the incidence angle thereby indicating the trioctahedral nature of these minerals. The effect is more pronounced in the saponite than in the hectorite, probably because of the substitution of some OH by F in the hectorite.

In the 2000-600 cm.$^{-1}$ region the samples were examined as films without any protection, and as disseminated KBr pellets in concentrations of 0.3 to 0.8 per cent. All the samples show a band at 1625 cm.$^{-1}$ characteristic of the adsorbed water (deformation frequency of the H-O-H vibration). There is strong absorption at 1000–1050 cm.$^{-1}$ associated with the Si-O bonds, and a medium band between 1075 and 1125 cm.$^{-1}$ which cannot be explained. Also in the montmorillonites and nontronites there is a relatively weak band at 840–850 cm.$^{-1}$. The absorption at 775 and 800 cm.$^{-1}$ is due to quartz impurity.

In montmorillonites with aluminum as a principal cation in octahedral positions there is a relatively strong band at 920 cm.$^{-1}$. In the nontronites this band is not present, but instead there is an absorption at 820 cm.$^{-1}$, the shift in frequency being produced by the substitution of iron for

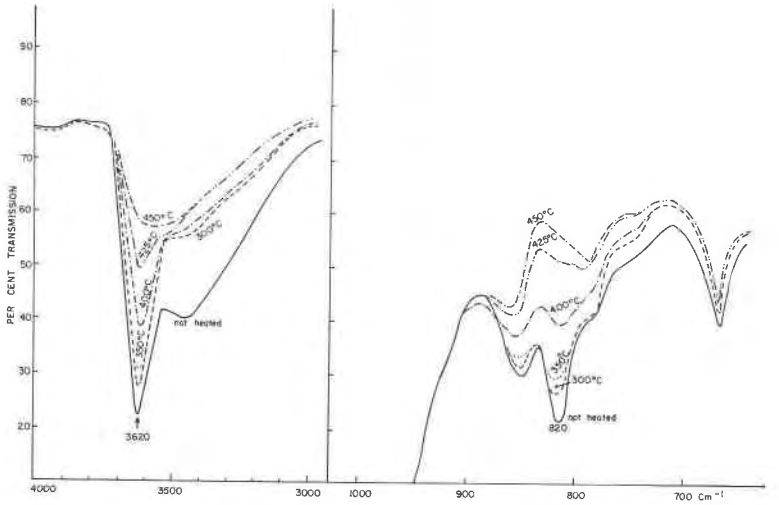

FIG. 23. Infrared absorption curves of nontronite (39) and after heating to temperatures indicated.

aluminum. To investigate this matter further spectra were obtained of montmorillonite and nontronite after heating to various temperatures up to 620° C. As shown in Figs. 22 and 23, the intensity to these two bands decreases regularly as the hydroxyls are lost. They must therefore, be related to the octrahedral layer, but at present it is not certain if these absorption bands correspond to a deformation vibration of the OH groups, or are associated with the vibration of the octahedra as a whole (O-Al-OH or O-Fe-OH vibrations).

In saponite and hectorite neither the 920 or 820 cm.$^{-1}$ band is present. Probably the strong absorption at about 650 cm.$^{-1}$ is the corresponding one in these minerals.

For the present study the salient conclusion from the infra-red data is that all the montmorillonites and the nontronite are dioctahedral. Any mixing of trioctrahedral crystallizations is believed to be very minor. The spectra do show slight variations in the 1200-600 cm.$^{-1}$ region which it is hoped future studies will relate to differences in the population of the tetrahedral and octahedral positions in the structure. In other words, it is not possible at the present time to relate these variations to differences in the type of montmorillonite, but there is considerable possibility that future investigations will permit such a correlation.

MICROSCOPIC STUDY AND OPTICAL PROPERTIES

Oriented aggregates produced by drying a suspension on a glass slide were examined with a petrographic microscope to determine the char-

acter of the aggregates and also, if possible, the optical properties of the montmorillonites.

In general the Wyoming-type montmorillonite shows much better aggregate orientation than the Cheto-type. The individual particles in the Wyoming-type aggregates are often too small to be seen individually and the aggregate has the appearance of the fragment of a single crystal. On the other hand, individual particles of the Cheto-type are easily visible in the aggregate which has a granular appearance. The uniformity of orientation of the individuals is much less in the Cheto-type than in the Wyoming-type. The particles of the Wyoming-type are not only smaller, but have aggregated together so perfectly that something akin to crystal growth has taken place.

As would be expected, the aggregates of the samples which are mixtures of the Wyoming- and Cheto-types are variable. Some are about like those of the Wyoming-type whereas other are distinctly granular. The aggregates of the miscellaneous type of montmorillonites are more like those of the Wyoming-type than the Cheto-type. Many of these samples provide aggregates which are composed of extremely small particles with a very high degree of uniformity of orientation. The sample of hectorite gives particularly excellent aggregates.

The optical properties were studied to determine if there was any consistent difference between values for the Cheto- and Wyoming-types. No such differences were found unequivocally and perhaps none are to be expected since, as Ross and Hendricks (1945) have shown, the indices vary with the iron content and as Mehmel (1937) has shown, the indices also vary with the content of magnesium. As both the iron and magnesium vary within the types, the influence of this variable might well conceal any variation between types. However, the data suggest that where the composition is similar the Wyoming type has slightly higher indices. Thus, sample 8, which is a Wyoming-type with a low iron content has a higher indice ($\beta = 1.530$) than sample 4 of the Cheto-type with a slightly higher iron content ($\beta = 1.520$). No satisfactory explanation can at the moment be offered for a possible consistent difference in optical properties from one type to the other.

Potassium and Magnesium Treatment

Samples of the various types of montmorillonite were treated with KCl (1N) and then washed until free of chloride. Diffraction diagrams were obtained on oriented slides after air drying with and without glycol treatment, and after oven drying and glycol treatment.

Wyoming-type samples, Fig. 24, collapsed to a c axis spacing of about 11.7 Å on air drying. Both the air dried and oven dried (at 100° C. for 2 hours) expanded to about 17.4 Å following glycol treatment. Therefore

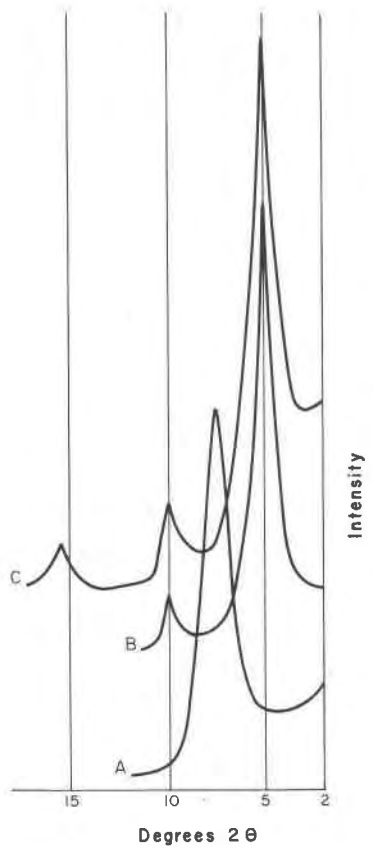

FIG. 24. *X*-ray diffraction data for Wyoming-type montmorillonite (10) treated with KCl. A—air dried, B—air dried and glycol treated, C—dried at 100° C. for 2 hours and glycol treated.

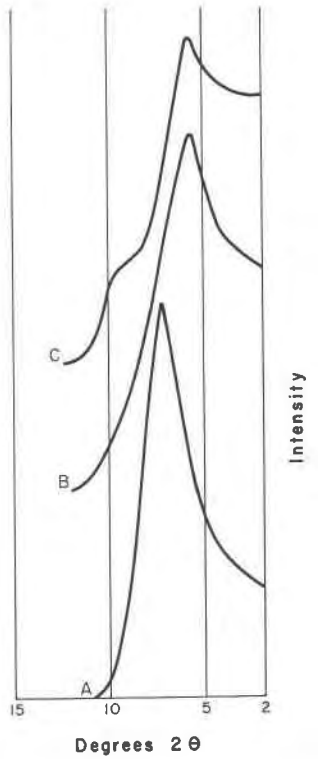

FIG. 25. *X*-ray diffraction data for Cheto-type montmorillonite (1) treated with KCl. A—air dried, B—air dried and glycol treated, C—dried at 100° C. for 2 hours and glycol treated.

it may be concluded that no permanent collapse of the structure or retardation of expansion was caused by potassium treatment of this type of montmorillonite.

The two samples of Cheto-type, Figs. 25 and 26, so treated collapsed on air drying to 12.1 and 11.9 Å. respectively. Following glycol treatment the air dried samples expanded to 15.5 and 14.7 Å, respectively. Glycol treatment of the oven dried samples produce material which expanded to about 15.5 and 14 Å, respectively. Results following the treatment of potassium chloride are therefore different for the two types of montmorillonite. This matter is being investigated further. Present data show

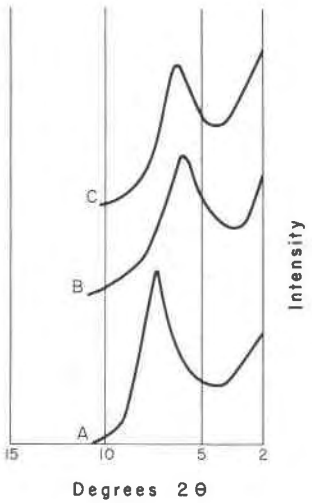

FIG. 26. *X*-ray diffraction data for Cheto-type montmorillonite (3) treated with KCl. A—air dried, B—air dried and glycol treated, C—dried at 100° C. for 2 hours and glycol treated.

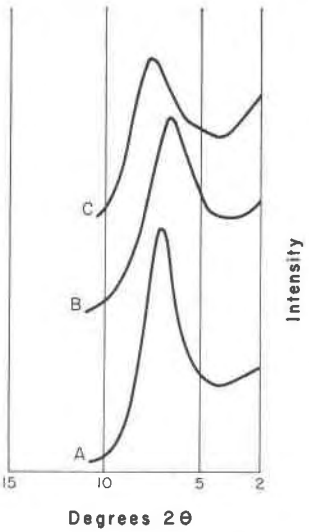

FIG. 27. *X*-ray diffraction data for iron-rich montmorillonite (37) treated with KCl. A—air dried, B—air dried and glycol treated, C—dried at 100° C. for 2 hours and glycol treated.

that the results are not the same for all montmorillonites derived from bentonites, and that the process must be used with caution in distinguishing expandable clay minerals derived from different parent materials (*e.g.* degraded micas versus montmorillonites from bentonites). It seems worthwhile to emphasize that the type of montmorillonite which shows no effect of potassium treatment, *i.e.* Wyoming type, is the one with a lower charge on the lattice and a lower cation exchange capacity. The type with a greater charge on the lattice shows retardation and reduction in amount of expansion, *i.e.* apparently in this type of montmorillonite enough potassium is held between the silicate layers to prevent complete expansion.

Miscellaneous sample 37 following potassium treatment shows, Figs. 26–27, a *c*-axis spacing of 12.5 Å without glycol treatment and 13.6 Å after glycol treatment. After oven drying the sample shows an expansion with glycol to only 11.6 Å. This sample has a larger amount of replacement within the octahedral positions than the Cheto-type samples, and as expected potassium treatment causes a greater reduction in expansion than for the Cheto-type samples.

The same samples were treated with magnesium chloride (1N) and then washed free of chloride. The results were the same for all the sam-

ples. Diffraction patterns obtained after air drying show a c-axis spacing of 13.8 Å. Following glycol treatment, the air dried samples and samples oven dried at 100° C. for 2 hours expanded to 17.2 Å. Thus the magnesium treatment has no effect in reducing the amount of expansion of the montmorillonites studied. The difference in the effect of potassium and magnesium is expected, since regardless of the charge, at least within the limits of the samples investigated, the size and coordination char-

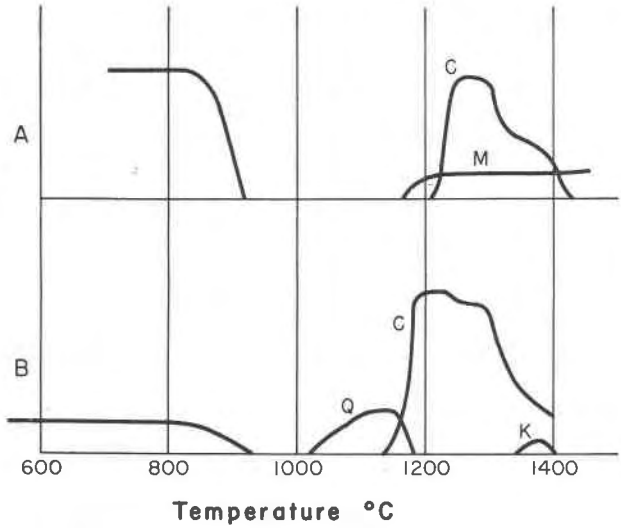

FIG. 28. High temperature phases developed by particle size fractions of a sample (29) composed of a mixture of Cheto- and Wyoming-type montmorillonites. A, Fraction <1 micron; B, Fraction 2–1 micron; Q, Beta Quartz; C, Beta Cristobalite; M, Mullite; K, Cordierite.

acteristics of the magnesium ion would not cause it to aid in restricting the expansion of dried montmorillonites. Further magnesium treatment is a safer way to distinguish expandable material derived from chlorite as compared to montmorillonite derived from volcanic ash than is potassium treatment in distinguishing expandable material derived from mica as compared to montmorillonites from bentonites.

FRACTIONATION OF THE SAMPLE COMPOSED OF MIXTURE OF TYPES

Sample 29, indicated as a mixture of the Wyoming- and Cheto-type montmorillonite was fractionated by centrifuging a dilute suspension of the minus 2 micron component into the fractions containing particles of 2—1 microns and minus 1 micron. It can be seen from Fig. 28 that the finer fraction gave high temperature phase characteristics of the Wyoming-

type, whereas the coarser fraction exhibited such characteristics of the Cheto-type. It may be concluded that in this sample at least the mixture is one of discrete particles. Also, as expected, the Wyoming-type dispersed into smaller particles than did the Cheto-type montmorillonite.

Discussion

The present investigation indicates that dioctahedral montmorillonites do not form a single continuous isomorphic series. Two different aluminous types have been found, Cheto- and Wyoming-types, which differ primarily in the population of the octahedral layer; notably in the relatively higher amount of magnesium in the Cheto samples.

It is noteworthy that the addition of magnesium to the Wyoming-type montmorillonite does not cause the development of high temperature phases characteristic of the Cheto-type (unpublished data). Also repeated leaching of the samples with HCl in order to remove most of the octahedral cations did not change the high temperature reactions of either type. It seems, therefore, that there are structural as well as compositional differences between the two types. The analytical data suggest that these differences are as follows:

The Cheto-type has relatively more substitution of aluminum by magnesium in the octahedral layer causing a greater charge on the lattice. Further, the replacements are relatively more regular, *i.e.* the position of the magnesiums is in a fairly definite pattern in the Cheto-type. If the magnesiums were randomly distributed, the particles would have some Mg-rich areas as well as some Mg-poor areas. Therefore, they would have high-temperature phases of both types; indeed, this never happens with properly sized and purified fractions. Also it is thought that some (probably a small number) of the silica tetrahedra are inverted in the Cheto-type. There does not seem to be a difference in the population of the tetrahedral positions in the two types.

Figure 29 shows an ideal arrangement of octahedral cations with one fourth of the aluminums replaced by magnesium. This is close to the average Cheto-type composition and it seems reasonable to think that this type of montmorillonite has the magnesiums arranged in such a pattern. Considering this pattern the typical properties of the Cheto-type montmorillonite can be explained. Thus, the exchange sites being on a hexagonal net, the same kind of symmetry can be expected in the stacking of the elementary silica layers. Some of the exchangeable cations can also act as bonds between the layers. The net result of these factors would be the larger particles characteristic of the Cheto-type, the more difficult complete dispersion, and the development of a mica-like structure following potassium treatment. On the contrary, in the Wyoming-type mont-

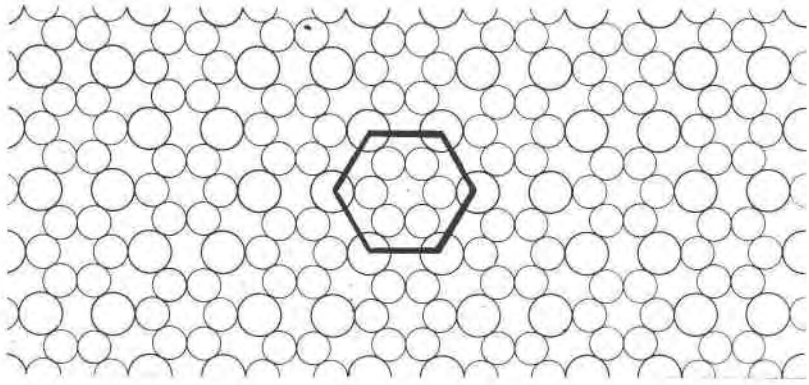

FIG. 29. Probable arrangement of octahedral cations in Cheto-type montmorillonite, showing suggested hexagonal arrangement of exchange sites. Large circles—Mg, small circles—Al.

morillonite, the exchange sites are randomly distributed, and no regular stacking and bonding of the silicate layers is to be expected. As a consequence, hydration and dispersion of the individual layers is relatively very easy.

The Cheto-type shows a greater loss of water in the 100–500° C. temperature interval which can be accounted for by some inversion of the silica tetrahedra. The hydroxyls of the exposed tips of the tetrahedra would probably be lost within this temperature interval.

No specific explanation can be offered for the variation in the dehydroxylation characteristics, i.e. dual versus single endothermic peak accompanying the reaction and the variation in intensity of the reaction. Samples with higher iron and magnesium contents have reactions of lesser intensity, so that variations in composition are a factor but structural attributes also are probably important. It seems likely that a dual peak means some sort of mixing of layers.

The intensities of the (001) reflections do not change on dehydroxylation of the Cheto-type samples whereas the relative intensities of these reflections do change for the Wyoming-type. It would seem likely that there would be less structural adjustment in the better crystallized Cheto-type with its regularity of substitution in the octahedral positions and hence less change in the intensity of the basal reflections accompanying the loss of hydroxyls.

The endothermic peak at about 900° C. varies in intensity and over a considerable temperature interval and is probably a matter of the abruptness of the loss of the montmorillonite structure causing it. For the Cheto-type the reaction is generally relatively intense in accordance

with the better crystallinity and hence the probable more abrupt loss of structure. The reaction for the Wyoming-type may be large or small, probably due to small variations in crystallinity and probably also to variations in composition. The intensity of the reaction decreases as the iron content increases, and in very iron-rich samples it is about absent. The presence of iron thus favors a gradual loss of the montmorillonite structure.

Electron micrographs show that the loss of the diffraction characteristics at about 900° C. is not accompanied by the complete loss of the external morphology, *i.e.* the flake shape of the units is still preserved. Data are not unequivocal, but the external form seems to be better preserved in the Cheto type than in the Wyoming-type montmorillonite. The reaction cannot be a complete structural breakdown but rather one in which the layer character is retained probably with lack of stacking order and some distortion in the *a* and *b* direction.

The formation of beta quartz from the Cheto-type probably involves whole reorganization of adjacent tetrahedral layers. It is thought that the presence of some inverted tetrahedra would favor the formation of this quartz phase which is not in the temperature domain of the formation of beta quartz as indicated in silica equilibrium diagrams. The postulated absence of inverted silica in Wyoming-type would explain the absence of a quartz phase from these montmorillonites (it has been pointed out that there is no difference in the composition of the tetrahedral positions in the two types). The differences in the temperature interval for various Cheto-type samples between the loss of montmorillonite diffraction and the formation of beta quartz and the variation in the intensity of the reaction accompanying the formation of quartz may be explained by variations in the amount of inverted tetrahedra and the consequent variation in the ease of formation of beta quartz.

The Wyoming-type montmorillonite shows a long temperature interval between the loss of montmorillonite diffraction and the formation of any high temperature phase. The absence of any inverted tetrahedra makes difficult the development of new phases. Cristobalite appears at a lower temperature in the Cheto- as compared to the Wyoming-type samples. That is, it appears at a lower temperature when formed by the inversion of beta quartz than when it develops directly from the silica of the montmorillonite structure.

At about 1200° C. mullite forms from the Wyoming-type samples. This phase does not form from the Cheto-type mineral as apparently magnesium in amounts in excess of about 1–2% MgO prevent the formation of mullite. Also, in the iron-rich samples, mullite does not appear so that small amounts of iron also block the formation of mullite. The

mullite that does form from the Wyoming-type montmorillonite probably is not pure aluminum silicate as the lattice parameters are slightly different from published values of pure material—in many instances it probably has about all the impurities that the structure will tolerate.

The intense exothermic peak shown on the differential thermal curves of the Wyoming-type samples at about 1000° C. is not accompanied by any crystalline phase detectable by *x*-ray diffraction. This reaction is interpreted as a consequence of a shift in bonding within the structure probably from face sharing octahedral units of dehydrated montmorillonite to the more stable edge sharing units which prevail in the high temperature structures that may form. This bonding shift is but one step in the development of new high temperature phases. A second step is the migration of cations into proper positions on a scale leading to crystal growth of a size detectable by *x*-rays. Higher temperature (about 1200° C.) is required to provide sufficient mobility of the cations so that this growth can take place. This second step may never take place if the composition is not proper for the specific network to form or if cations are present which block the growth or break up the network at relatively low temperatures. The potassium ion for example substantially inhibits the formation of any high temperature phase from the montmorillonite minerals (Kulbicki and Grim, 1957).

The phases that form at temperatures below about 1200° C., *i.e.* the beta quartz and cristobalite from it, form at this relatively low temperature because of their structural relation to the silica part of the montmorillonite structure. The first or nucleation stage of phases that appear prominently above about 1200° C. is closely dependent on the structure of the original mineral. Thus the arrangement of the magnesiums in the octahedral layer of the Cheto-type is such that the nucleation of cordierite is favored. The development of the high temperature phases beyond the nucleation stage is determined largely by the bulk composition of the material.

The presence of cristobalite in the unfired clay has no effect on the formation of high temperature cristobalite. This indicates that the new cristobalite is formed directly from montmorillonite rather than by a complete breakdown of a montmorillonite structure and then a regrouping around the primary cristobalite. That is, the formation of the new cristobalite is a solid state reaction from the montmorillonite.

The miscellaneous types of aluminous montmorillonites differ from the Wyoming-type only in the formation of a small amount of beta quartz. This can be explained by a varying small amount of inversion of the silica tetrahedra in these samples.

Nontronite and the very iron-rich montmorillonites only yield a silica

phase (cristoballite) at elevated temperatures. Iron apparently in substantial amounts blocks the development of any other crystalline phase.

For the trioctahedral magnesium-rich montmorillonites and talc, enstatite develops before the montmorillonite structure is completely lost and without any accompanying thermal reaction. This suggests a gradual breakdown of the structure of the original mineral with gradual growth from the debris of the enstatite—unlike the solid state reactions for the dioctahedral forms. In some cases, cristoballite develops at very high temperatures from the left over silica. The reason for the development of little or no cristoballite in some cases (hectorite) and much for other minerals (saponite) is not clear. The elongate structure of the hectorite as compared to the flake-shape of the saponite may be significant.

References

Byrne, P. J. S. (1954), Some observations on montmorillonite-organic complexes: *Proc. Second Nat. Clay Conference Pub.* **327,** *U. S. Nat. Acad. of Sci.*, 241–253.

Deuel, H., Huber, G., and Iberg, R. (1950), Organische Derivate von Tonmineralien: *Helv. Chim. Acta*, **38,** 1229–1232.

Edelman, C. H., and Favejee, J. Ch. L. (1940), On the crystal structure of montmorillonite: *Zeit. Krist.*, **102,** 417–431.

Grim, R. E. (1934), The petrographic study of clay minerals—A laboratory note: *Journ. Sed. Petrol.*, **4,** 45–46.

——— and Rowland, R. A. (1942), Differential thermal analyses of clay minerals and other hydrous materials: *Am. Mineral.*, **27,** 746–761, 801–818.

Hendricks, S. B. (1942), Lattice structure of clay minerals and some properties of clays: *Jour. Geol.*, **50,** 276–290.

Hofmann, U., Endell, K., and Wilm, D. (1933), Kristallstruktur und Quellung von Montmorillonit: *Zeit. Krist.*, **86,** 340–348.

Jonas, E. C. (1955), The reversible dehydroxylization of clay minerals: *Proc. Third Nat. Clay Conf., Publ.* **395,** *U. S. Nat. Acad. of Sci.*, 66–72.

Kulbicki, G., and Grim, R. E. (1957), Etude des Reactions de Hautes Temperatures dans les Mineraux Argileux au Moyen des Rayons X: *Bull. Soc. France Ceramique*, **36,** 21–28.

MacEwan, D. M. C. (1951), The Montmorillonite minerals, "*X*-ray Identification and Structure of the Clay Minerals." Monograph Min. Soc. Great Britain, 86–137.

Marshall, C. E. (1935), Layer lattices and base-exchange clays: *Zeit. Krist.*, **91,** 433–449.

McAtee, J. L. (1958), Heterogeneity of montmorillonites: *Proc. Fifth Nat. Clay Conf., Publ.* **566,** *U. S. Nat. Acad. of Sci.*, 270–288.

McConnell, D. (1950), The crystal chemistry of montmorillonite: *Am. Mineral.*, **35,** 166–172.

Mehmel, M. (1937), Beitrage zur Frage des Wasserhaltes der Minerale Kaolinit, Halloysit und Montmorillonit: *Chem. Erde*, **11,** 1–16.

Ross, C. S., and Hendricks, S. B. (1945), Minerals of the montmorillonite group: *Prof. Paper* **205-B,** *U. S. Geol. Survey*, 23–79.

Serratosa, J. M., and Bradley, W. F. (1958), Infra-red adsorption of OH bonds in micas. *Nature*, **181,** 111.

Manuscript received January 18, 1961.